# Electrical and Electrochemical Characterization of Electroconductive PPy-p(HEMA) Composite Hydrogels

Sean Brahim[†], Gymama Slaughter[†], Anthony Guiseppi-Elie[†‡*]

Departments of [†]Chemical Engineering and [‡]Emergency Medicine and [†]The Center for Bioelectronics, Biosensors and Biochips (C3B), Virginia Commonwealth University, School of Engineering, P. O. Box 843038, 601 West Main Street, Richmond, Virginia 23284-3038

## ABSTRACT

Two groups of polymers that have been the focus of widespread research are hydrogels and conducting electroactive polymers (CEPs). 'Intelligent' hydrogels are highly hydrophilic, cross-linked polymers possessing hydration properties that change in response to specific environmental stimuli such as pH, ionic strength, chemical species, magnetic fields, etc. Conducting electroactive polymers such as polypyrrole, polyaniline and polythiophene are highly conjugated, redox-active polymers with electrical and optical properties that change through many orders of magnitude depending upon redox state (doping). We have formed composites of inherently conductive polypyrrole within highly hydrophilic poly(hydroxyethyl methacrylate)-based hydrogels. These materials retain the hydration characteristics of hydrogels as well as the electroactivity and electronic conductivity of CEPs and are thus called 'electroconductive hydrogels'. The electrical and electrochemical properties of these polymer composites have been investigated. The electrochemical characteristics observed by cyclic voltammetry suggest less facile reduction of PPy within the composite hydrogel compared to electropolymerized PPy, as shown by the shift in the reduction peak potential from –472 mV for electropolymerized polypyrrole to -636 mV for the electroconductive composite gel. The network impedance magnitude for the electroconductive hydrogel remains quite low, ca. 100 Ohms, even upon approach to DC, over all frequencies and at all offset potentials suggesting retained electronic (bipolaronic) conductivity within the composite.

**Keywords:** electroconductive, hydrogel, polypyrrole, electroactive polymers, polymer composites, cyclic voltammetry, electrochemical impedance spectroscopy

## 1. INTRODUCTION

The recent emphasis on materials science and chemistry has opened new approaches to analytical sensing, influencing the design of sensors, particularly those using electrochemical or spectroscopic transduction methods. Polymeric materials have played important roles in the development of sensors for their ability to increase analyte sensitivity and selectivity via phase-transfer chemistry. Conducting electroactive polymers (CEPs) have been fascinating many scientists worldwide with their interesting electronic properties and sensing capabilities. Innumerable applications of these polymers such as thin films for batteries, sensors, ion selective electrodes and solid-state devices have been extensively reported since the early 1990s[1-3]. Scientists now believe that with the explosive research and advances in electroactive polymers, these materials could, in fact, revolutionize robotics and biomedical devices by designing more life-like prosthetic limbs, durable artificial muscles, and more efficient implantable microdelivery systems[4]. Conducting polymer composites have been fabricated combining polypyrrole and polyaniline with a host of polymers such as poly(vinyl chloride)[5], polycarbonate[6], poly (vinyl alcohol)[7], poly (acrylonitrile)[8], polyamides and imides[9], poly(ether ketone)[10], nafion[11], and rubber[12]. Each of these efforts has significantly modified the physical and mechanical properties of the conducting polymer component and have rendered them suitable for application in different devices. A great number of biological materials can be immobilized by

* guiseppi@vcu.edu; phone: 1 804 827-7016; fax: 1 804 827-7029; http://www.biochips.org/



Smart Structures and Materials 2003: Active Materials: Behavior and Mechanics,
Dimitris C. Lagoudas, Editor, Proceedings of SPIE Vol. 5053 (2003)

blending them with these composites to form new biocomposite materials. These biocomposites not only act as reservoirs of the biological material but may also contain catalysts, mediators and cofactors that improve the response of the resulting electrochemical sensors[13].

Another interesting class of polymer that has attracted much research and investigation is hydrogels. Hydrogels, as the name implies, are three-dimensional hydrophilic polymer networks capable of imbibing large quantities of water yet remaining insoluble and preserving their shape. The so-called 'responsive' hydrogels are materials whose properties change in response to specific environmental stimuli such as pH, temperature, ionic strength, etc[14]. The utility of hydrogels as sensors, by themselves or chemically modified, has been examined by several research groups. Hydrogels have been employed as the sensing layer in amperometric[15], potentiometric[16], conductimetric[17], and fibre-optic sensors[18]. The attractive feature of using hydrogels as the immobilizing matrix for biomolecules in the fabrication of sensing devices is that the high water content affords the immobilized biomolecule a microenvironment that resembles that of the solution-borne counterpart.

We have previously combined these two classes of polymer into one composite material that we call 'electroconductive hydrogels'. Such composite membranes were used to immobilize oxidase enzymes (glucose, cholesterol, and galactose) and subsequently evaluated as amperometric enzyme biosensors[19-21]. We now report on the electrical and electrochemical characterization of these composite polymer membranes. The electroconductive hydrogel of this study consists of cross-linked p(2-hydroxyethyl methacrylate) (the hydrogel component) within which polypyrrole (the electrically conducting component) has been electrochemically polymerized.

## 2. EXPERIMENTAL

### 2.1. Materials

The monomer, hydroxyethylmethacrylate (HEMA), was obtained from Polysciences Inc., Warrington, PA, while the cross-linker tetraethyleneglycol diacrylate (TEGDA), inhibitor remover columns, pyrrole monomer (Py), and photoinitiator dimethoxyphenyl acetophenone (DMPA) were all obtained from Aldrich Co. (Milwaukee, WI). Platinizing solution (YSI 3140) was purchased from YSI, Inc. (Yellow Springs, OH). The HEMA and pyrrole monomers were both vacuum distilled before use (1.3 mm Hg, 80ºC and 3.5 mm Hg, 60ºC, respectively). All other reagents used were of the Analytical Reagent grade (Aldrich Co.) and were used without further purification. The working electrodes used for all electrochemical characterization studies were microlithographically fabricated interdigitated microsensor electrodes (IMEs) (part number IME 1050.5-M-Pt-U) that were purchased from ABTECH Scientific Inc. (Richmond, VA). Each borosilicate glass chip consisted of a pair of opposing electrodes comprising 10 mm wide platinum digits that were ca. 5 mm long and separated by 10 mm wide free spaces. There were 50 digits on each electrode bus that established a tortuous path of 49.60 cm of exposed glass surface between the digits. Planar indium-tin oxide electrodes (PITOE 150: 0.9cm x 5.0cm x 0.05cm) for UV-VIS spectroscopy and spectroelectrochemistry were purchased from ABTECH Scientific, Inc. (Richmond, VA). Quartz crystal oscillators having gold driving electrodes were purchased from International Crystal Manufacturing Co., Inc. (Oklahoma City, OK).

### 2.2. Methods

#### 2.2.1. Formulation of electroconductive hydrogels

The platinum electrodes were washed in boiling trichloroethylene, followed by boiling acetone, 3 minutes in each solvent, then ultrasonically washed in isopropanol followed by distilled water. This was followed by treatment at 60°C for 30 seconds with a solution comprising a 1:1:5 volume ratio of aqueous ammonia (0.1M), hydrogen peroxide (20% volume) and distilled water. The electrode surfaces were then rinsed ultrasonically in DI water. An active window of area 0.25 $cm^2$ was formed using adhesive backed polyimide tape on the surface of the clean, platinum electrode. The composition of the electroconductive hydrogel that was selected corresponded to the formulation used in the construction of amperometric biosensors[19]. This formulation consisted of the monomers HEMA:TEGDA:Py in a ratio 85:10:05 vol%. The acrylate monomers HEMA and TEGDA were first mixed together and used as the receiving mixture to dissolve the photoinitiator. An appropriate quantity (typically 3 μL) of the formulated gel-monomer mixture was then applied to the window and a thin film cast over the working electrode area by spin coating at ca. 300 r.p.m for 5 seconds. The mixture was immediately irradiated with U.V. light (366 nm, 2.3 watts/$cm^2$, Spectroline Model 330844) for 45 minutes under an inert argon atmosphere to effect

polymerization of the hydrogel component. The electrode was then immersed into 3 mL of a deaerated phosphate buffered KCl solution (0.1M $NaH_2PO_4$ containing 0.1M KCl, pH 7.2) that was saturated with pyrrole monomer (ca. 0.4 M). The polypyrrole component of the composite membrane was deposited within the interstitial spaces of the pre-formed hydrogel network by potentiostatic electropolymerization (+0.85 V *vs.* Ag/AgCl) for 100 seconds. The electrodes were then rinsed with phosphate buffer (0.1M, pH 7.0) to remove any residual monomer. Finally, the composite poly(HEMA)-polypyrrole film was further extensively oxidized at +0.7 V *vs.* Ag/AgCl (the working potential typically required to oxidize enzymatically generated $H_2O_2$) until the background current fell below 1.0 μA. When not in use, the electrodes were desiccated and stored at 4ºC in the absence of buffer.

### 2.2.2. Characterization of the composite polymer membranes

For all electrochemical characterization studies (EIS and cyclic voltammetry) composite membranes of the electroconductive hydrogels were grown as outlined above on cleaned microlithographically fabricated interdigitated microsensor electrodes (IMEs). Prior to membrane deposition, electrode platinization was performed via controlled potential coulometry (-50 mV *vs.* Ag/AgCl, 3 M $Cl^-$ ref. electrode for 10 sec.) in the platinizing solution. The set-up for three-electrode electrochemistry consisted of a Perkin-Elmer Princeton Applied Research M273 Potentiostat/Galvanostat linked to a Gateway PC and controlled by EG&G M272 software. Cyclic voltammetry, amperometry, electrochemical polymerization and coulometry were performed in a standard three-electrode cell with a miniature Ag/AgCl, 3M $Cl^-$ reference electrode (RE 803; ABTECH Scientific, Inc.) and a platinum mesh counter electrode. Three-electrode electrochemical impedance spectra (10 mV amplitude; sine wave; 1 mHz - 60 kHz; 25 ± 1 °C) were obtained using a Perkin-Elmer Princeton Applied Research M273 Potentiostat/Galvanostat coupled with a Solartron Schlumberger 1250 Frequency Response Analyzer (FRA). The FRA was used in single-sine mode to cover the range 1 Hz - 60 kHz and the M 273 was used in multi-sine mode to cover the range 1 mHz - 1 Hz. The EG&G M398 software was used for data capture, data merging and analysis. Two-point electrical resistance measurements of the polymer membranes were made using a Keithley Model 2000 Multimeter. Time-dependent UV-Vis spectra of the growing polypyrrole content of the composite membranes were performed on a Perkin Elmer Lambda 40 UV/Vis Spectrometer. Planar indium-tin oxide electrodes consisting of borosilicate glass having one side coated (10 Ohms/sq) were used as the substrate to support chemical oxidative growth of the polypyrrole component of the composite polymer membranes. Optical density measurements (300 - 800 nm) were obtained for electroconductive hydrogels containing polypyrrole that was polymerized for different oxidation times (45, 120, 180 s). To quantify the actual mass of polypyrrole that was deposited within the hydrogel network, frequency dependant mass changes were performed before and after electropolymerization of the pyrrole monomer on AT cut quartz oscillators with gold electrodes and using a quartz crystal microbalance (QCM). For gravimetric analyses using the quartz crystal microbalance, the shift of resonant frequency (Δf) was measured using a high-resolution programmable model PM 6680B Timer/Counter (Fluke, Everett, WA) and TimeView software.

## 3. RESULTS AND DISCUSSION

### 3.1. Cyclic Voltammetry

Cyclic voltammograms were obtained in simple phosphate buffered KCl (0.1 M in each component; pH = 7.2) for each of the following polymer systems; (i) the UV polymerized p(HEMA)-based hydrogel containing no polypyrrole, (ii) electropolymerized polypyrrole ($Cl^-$ counter anion) without any hydrogel, and (iii) the electroconductive composite membrane comprising polypyrrole electropolymerized within the UV polymerized p(HEMA)-based hydrogel. As expected, the cyclic voltammogram for cross-linked p(HEMA) hydrogel, shown in Figure 1.a, shows no redox peaks associated with the polymer over the potential investigated. With respect to electropolymerized polypyrrole (Figure 2), well-resolved voltammograms were obtained at the different scan rates investigated (10 - 100 mV/s). Peak separations between anodic and cathodic peak potentials ($\Delta E_p$) were 110, 84, 138 and 200 mV over the four scan rates of 10, 20, 50 and 100 mV/s investigated. At the highest scan rate of 100 mV/s, well-defined oxidation and reduction peaks were observed at -266 and -472 mV, respectively. The current ratios of cathodic and anodic peak currents, $I_{pc}$ / $I_{pa}$, did not deviate significantly from 1 suggesting redox reversibility. The formal potential, E°', was observed to shift by 34 mV to more negative potential (-335 to -

369 mV) upon increasing the scan rate from 10 to 100 mV/s. Cyclic voltammograms for the composite electroconductive hydrogel *after* electropolymerization of the incorporated pyrrole monomer at +0.85 V *vs.* Ag/AgCl for 100 s but *before* extensive oxidation at +0.7 V *vs.* Ag/AgCl showed retained electroactivity (Figure 3). Both anodic and cathodic peak currents were slightly reduced compared to those for electropolymerized polypyrrole. Anodic and cathodic peak potential separations, however, were now observed to increase to 178, 166, 256 and 336 mV for their respective scan rates of 10, 20, 50 and 100 mV/s, almost double the $\Delta E_p$ at corresponding scan rates for electropolymerized polypyrrole. The current ratios, $I_{pc}$ / $I_{pa}$, averaged around 1.4 over the four scan rates investigated suggesting that the cathodic reaction is more facile than the anodic reaction. Likewise, the formal potential of the composite shifted to more negative values, -401 to -468 mV, upon increasing the scan rate to 100 mV/s. When we compare the polypyrrole with the PPy-p(HEMA) composite, for example, at 100 mV/s, there was a decrease in both oxidation and reduction peak potentials compared to polypyrrole; from -266 to -300 ($E_{ox}$) and –472 to -636 mV ($E_{red}$), respectively. We find that the increase in $\Delta E_p$ arises because of the shift in the cathodic peak to more negative potentials. The overall impact of composite formation is to force the cathodic reaction to more negative potentials suggesting less facile egress of anions or ingress of cations under the swollen conditions of the hydrogel composite.

After oxidizing the electroconductive hydrogel for one hour at +0.7 V *vs.* Ag/AgCl, a process we call *extensive oxidation*, the composite polymer still showed electroactivity (Figure 4). Compared to the voltammograms for the composite membrane obtained before extensive oxidation (shown in Figure 3), there was now a reduction in the cathodic peak current but a corresponding increase in the anodic peak current. $\Delta E_p$ values were now significantly less than those for the composite membrane obtained before extensive oxidation (2, 168 and 248 mV at 20, 50 and 100 mV/s). The formal potential following *extensive oxidation* ranged from -211 to -336 mV for the scan rates 20 to 100 mV/s. At the highest scan rate of 100 mV/s, there was an increase in both $E_{pa}$ and $E_{pc}$ to -212 and -460 mV, respectively, even higher than those observed for electropolymerized polypyrrole. Interestingly however, after *two* hours of extensive oxidation at +0.7 V *vs.* Ag/AgCl, there was a complete loss of electroactivity as shown by the voltammogram in Figure 1.b.

It is evident that the electroactivity of these composite hydrogels is solely due to the presence and intimate association of the electrically conducting component, polypyrrole, within the hydrogel network. The loss of electroactivity after extensive oxidation is a phenomenon that suggests an inherent change in the backbone structure of the polypyrrole component. Several authors have reported on the overoxidation of polypyrrole as a process that disrupts the conjugation of the conducting polymer while maintaining the integrity of the polymer network and morphology[22-24]. Christensen and Hamnett[25] investigating the overoxidation of polypyrrole in aqueous solution found that overoxidation commences at potentials just greater than +0.7 V *vs.* Ag/AgCl. Such oxidizing potentials lead to ketone groups forming on the polypyrrole backbone. It is believed that the extensive oxidation of the electroconductive hydrogels in this study (to achieve steady low baseline currents) also results in the disruption of conjugation throughout the polymer by the generation of anionic groups with high electron density such as carbonyl functionalities in the polypyrrole backbone. This consequent disruption of conjugation may account for the observed loss of electroactivity with the extensively oxidized electroconductive hydrogels.

### 3.2. Electrochemical Impedance Spectroscopy

Both electroactive forms of the polymer systems under study (electropolymerized polypyrrole and the electroconductive hydrogel before extensive oxidation) were subjected to frequency-dependent impedimetric analyses at different inquiring or offset potentials. The three potentials that were selected for each polymer were i) the formal potential, $E^{o'}$, ii) $E^{o'} - \Delta E_p$, and iii) $E^{o'} + \Delta E_p$. The three-electrode impedance measurements were performed on the polymer membranes in phosphate buffered KCl solution in two different ways. The first was with a separate external counter electrode placed in solution and with the pair of interdigitated microsensor electrodes shorted to serve as a single working electrode, that is, *across* the polymer membrane. The second was with no external counter electrode and with one member of the pair of interdigitated microsensor electrodes serving as the counter electrode, that is, *within* the polymer membrane. The resulting magnitudes of the Bode plots for electropolymerized PPy-Cl are shown in Figure 5. The insets of Figure 5 illustrate the electrode arrangements.

For polypyrrole measured *within* the film (Fig. 5B), there was almost complete super positioning of the impedance magnitude, $|Z|$, and phase angle, $\theta$, at all potentials and across the entire frequency range interrogated. Thus, regardless of whether polypyrrole was in a reduced state (-575 mV), oxidized state (-163 mV), or in an intermediate redox state (-369 mV),

there was no observable significant impedance difference in the polymer at these different potentials. Sweeping over the frequency range from low (0.1 mHz) to high (60 kHz) was accompanied by an inherent decrease in network impedance by 3 orders of magnitude. The impedance upon approaching DC was in all cases ca. 100 kOhms.

For polypyrrole measured *across* the film (Fig. 5A), there was considerable variation of the impedance magnitude, $|Z|$, and phase angle, $\theta$, with the impressed or offset potential. In the frequency range approaching DC, it was observed that the network impedance with the highest value was established with polypyrrole in the reduced state (-575 mV), corresponding to the polymer in the electrically insulating state. There was a corresponding slight reduction in the peak phase angle at this reducing potential, from ca. 72° for polypyrrole measured *within* the film to 66°. Moreover, the peak phase angle was now shifted slightly to a lower frequency (< 1 Hz) compared to the *within* film measurement. Both intermediate redox and fully oxidized states of polypyrrole resulted in similar network impedance values in this frequency range. At frequencies between 0.01 Hz and 100 Hz, the network impedance magnitude displayed the most variation, with the largest impedance magnitude observed for polypyrrole in the oxidized state (-163 mV). The corresponding phase plot showed a significant reduction in peak phase angle at this potential of ca. 25° compared to the *within* film measurement. This peak phase also shifted considerably to ca. 100 Hz compared to 1 Hz for the corresponding *within* film arrangement. At the formal potential (-369 mV), the network impedance magnitude was intermediate between that for the system containing electrically conducting and insulating polypyrrole, displaying the least sloping profile. The resulting phase plot showed the appearance of three peak phase angles; the first occurred at 1 mHz, corresponding to an angle of ca. 72°, the second peak of ca. 19° occurred near to 1 Hz, and the third peak phase angle of 20° occurred at ca. 100 Hz. The second and third of these three peak phase angles correspond to those seen in the system containing reduced and oxidized polypyrrole, respectively. At the high end of the frequency range (> 100 Hz), impedance magnitudes at all potentials investigated approached the same value of ca. 200 Ohms, higher than that recorded for the system containing polypyrrole when measured *within* the film.

For the system containing the electroconductive hydrogel and measured *across* the gel (Figure 6A), the resulting impedance magnitude profiles at the three different potentials resembled those for electropolymerized polypyrrole in the same arrangement. The profile for the reduced form of the electroconductive hydrogel composite at -800 mV exhibited almost identical shape, slope and magnitude of change as that measured for the reduced form of the electropolymerized polypyrrole. The phase angle profile at –800 mV was also identical to that for the system containing electropolymerized pyrrole, with a peak phase of ca. 68° occurring at just under 1 Hz. The other two impedance magnitude profiles corresponding to oxidized gel (-132 mV) and gel in an intermediate redox state (-468 mV) displayed an impedance pattern similar to the respective redox states of polypyrrole. Between the frequency range 0.1 – 1000 Hz, the oxidized form of the electroconductive hydrogel exhibited the highest network impedance, with the intermediate redox state having network impedance magnitudes between the oxidized and reduced forms of the gel. Contrary to the phase angle plots obtained for oxidized and intermediate redox polypyrrole, however, corresponding forms of the electroconductive hydrogel both showed peak phase angles of 35° and 42° respectively at ca. 1 Hz.

When the network impedance magnitude is measured *within* the electroconductive membrane there is again no difference among the various potentials as seen in Figure 6B. However, it is very interesting to note that the impedance magnitude over all frequencies remains quite low, ca. 100 Ohms, even upon approach to DC, at all offset potentials. Ait is noteworthy that bare platinum electrodes when placed in the buffer solution produce an impedance of $5 – 7 \times 10^4$ ohms. Thus, regardless of whether the polypyrrole component is measured under presumed electrically insulating (-800 mV), electrically conducting (-132 mV), or in an intermediate (-468 mV) conditions, the impedance of the network is not impacted. The corresponding phase angle plot reflects this with an almost featureless profile over the entire frequency range investigated. We believe that under these conditions the network impedance is dominated by the electronic conductivity of the polypyrrole component of the composite. With ohmic contacts at both electrodes, the electronic conductivity is not influenced by ionic conductivity that is normally required to support oxidation and reduction of the PPy component.

### 3.3. I - t plots and UV-Vis spectra

During the extensive oxidation step, which occurs in phosphate buffered KCl, the anodic current *vs.* time plot obtained was one of increasing current magnitude leading to a maximum followed by a gradual fall to low current values and

eventually to a steady or background current value, typically 20 μA/cm$^2$ after ca. 60 min. This suggests that during this process the polypyrrole component continued to form from unreacted pyrrole monomer that partitioned from the pyrrole solution and contained within the preformed hydrogel membrane. The gradual fall in anodic current signals an approach to completion of electropolymerization and the onset of oxidative degradation reactions that results in an approach to background current values. Further evidence to support this was obtained from spectroelectrochemical studies performed on composite membranes cast onto ITO plates and subjected to different pyrrole oxidation times. Figure 7 clearly shows the progressive augmentation of a single absorbance band at 325 nm with increased oxidation time, suggesting further oxidative polymerization of unreacted pyrrole monomer and polypyrrole polymer formation even after 180 s of oxidation.

### 3. 4. Electrical resistance measurements

Both the p(HEMA) and PPy-p(HEMA) composite hydrogels were separately cast over the interdigitated area of an IME and the electrical resistance of the membranes measured. The dry, unswollen hydrogel gave an average resistance measurement of 7x10$^6$Ω. When swollen in 0.1M phosphate buffered KCl solution, pH 7.2, the resistance decreased dramatically by six orders of magnitude to 350 Ω (n = 5). This is due to the partitioning of ions into the gel as it hydrates and swells in the buffer. Following electropolymerization of polypyrrole, but before extensive oxidation, the electroconductive hydrogel had a mean resistance of 58 Ω (n = 5) which increased to 97 Ω after 3 hours of oxidation at + 0.7 V *vs.* Ag/AgCl. The 6-fold reduction from 350 Ω to 58 Ω arises from the electronic (bipolaronic) contribution of the conducting electroactive PPy component to the composite. The subsequent 1.7-fold increase (58 Ω to 97 Ω) following extensive oxidation at + 0.7 V supports a loss of conductivity possibly due to disruption of conjugation throughout the polypyrrole structure. It is noteworthy that the resistance does not return to the original resistance of the pure hydrogel suggesting that the composite is uniquely modified by the electropolymerization and subsequent extensive oxidation.

### 3. 5. QCM

The gravimetric quantity of polypyrrole that was electrochemically deposited within the hydrogel network from a starting formulation of 85:10:05 vol% HEMA:TEGDA:Py was determined using the quartz crystal microbalance sensor. We have treated the shift in resonant frequency of the oscillator following polymer formation as a pure *mass* accumulation, with the QCM sensor operating in the gravimetric regime. It should be noted that the mass effect is one but not the only effect that can significantly impact the acoustic behavior of the QCM sensor. The second important contribution is from the film modulus manifested as a measure of the viscoelastic properties of the coating. With increasing thickness, the viscoelastic properties of the coating gain influence on the piezoelectric sensor response and the sensor then approaches the non-gravimetric regime. To quantify the viscoelastic contributions from the coating, one can make use of the relation between change in motional resistance (ΔR) and resonant frequency ($\Delta f_o$) of the piezoelectric quartz crystal (PQC) due to net changes in the coating's density and viscosity[26, 27]:

$$\Delta R = \frac{4\pi\pi_q \Delta f_o \sqrt{f\mu_q}}{\sqrt{c_{66} f_{og}}} \approx -4\pi\pi_q \Delta f_o$$

where $f_{og}$ and $f_o$ are the resonant frequency of the PQC in air and liquid, $L_q$ is the motional inductance in air, $\mu_q$ is the shear modulus for AT-cut quartz (2.947 x 10$^{10}$ N/m$^2$), $c_{66}$ is the lossy piezoelectric stiffened elastic constant (2.957 x 10$^{10}$ N/m$^2$), and f can be approximated by $f_o$ in the calculation with an error less than 0.3%.

The measured average resonant frequency change, Δf, upon UV polymerization of the hydrogel component was -49.6 kHz (n = 25). Assuming the QCM sensor to be operating in the gravimetric regime, this change in resonant frequency of the quartz crystal resonator following polymerization of the hydrogel was used as a crude measure of mass change using Sauerbray's fundamental equation:

$$\Delta m = \frac{\Delta f \left[ A \sqrt{\mu \rho} \right]}{- 2 f_o^2}$$

where $f_o$ is the resonant frequency of the fundamental mode of the crystal, A is the area of the gold driving electrodes of the crystal (0.392 $cm^2$), m is the shear modulus of quartz (2.947 x $10^{10}$ $g/cm \cdot s^2$), and r is the density of the crystal (2.684 $g/cm^3$). Substitution gives a mass change of 0.01363 mg for the p(HEMA) hydrogel. Next, the electrochemical growth of polypyrrole from the pyrrole monomer that was seeded within the cross-linked p(HEMA) network resulted in an average resonant frequency change of -83 kHz (n = 25). This yielded a mass change of 0.00923 mg upon electropolymerization of the incorporated pyrrole monomer for 100 s at +0.85 V *vs.* Ag/AgCl, which corresponds to ca. 40 % by weight of the composite electroconductive polymer.

## 4. CONCLUSIONS

The intimate combination of hydrogels with conducting electroactive polymers has spawned a useful composite biomaterial with applications in bioelectronics and bioelectrochemistry. These polymers have been demonstrated as transducer-active, sensory membranes for biosensors, electronic noses and as actuators in artificial muscles. The electroconductive hydrogels demonstrate enhanced redox switching speeds and retained bioactivity and these materials have been used as bioactive membranes in amperometric biosensors for glucose, cholesterol and galactose. Electrochemical polymerization of the pyrrole monomer contained within the hydrogel network resulted in a conducting electroactive polymer that was grown under continuous oxidizing conditions. The electrochemical characteristics observed by cyclic voltammetry suggests less facile reduction of PPy within the composite hydrogel compared to electropolymerized PPy. This likely arises from the need to transport fully solvated anions out or solvated cations into the gel that may be parts of extensive ionic clusters or cages. Figure 8 illustrates this concept. Further extensive oxidation of the composite membrane at +0.7 V *vs.* Ag/AgCl resulted in an inherent loss of electroactivity as well as decrease in electrical conductivity. The electropolymerization and subsequent extensive oxidation of the polypyrrole component of the composite does not just inactivate the polypyrrole component, as the resulting composite has unique electrochemical and electrical properties. Further research with these interesting composite materials include optical characterization, formulation of a hydrogel composition containing derivatized polypyrrole covalently attached as a pendant to the cross-linked network, and the inclusion of a phosphorylcholine containing methacrylate as co-monomer for *in vivo* sensing applications.

## ACKNOWLEDGMENTS

The authors acknowledge the financial support of the VCU Center for Bioelectronics, Biosensors and Biochips (C3B) and the Virginia Center for Innovative Technology (CIT BIO-99-010). We thank Dyer Narinesingh and Dow Maharajh of the Department of Chemistry, The University of the West Indies, for useful discussions.

## REFERENCES

1. M. Gerard, A. Chaubey, B.D. Malhotra, "Application of conducting polymers to biosensors", *Biosens Bioelectron*, **17**, 345-359, 2002.
2. M. Angelopoulos, "Conducting polymers in microelectronics", *IBM J. Res. Dev*., **45**, 57-75, 2001.
3. Y. Osada, D.E.D. DeRossi, "Polymer Sensors and Actuators", R.A. Bailey, K.C. Persaud, eds., 149-181, Springer: Berlin, 2000.
4. G.T. Huang, "Electroactive Polymers", *Technology Review*, **December 2002 / January 2003**, 32, 2003.
5. O. Niwa, M. Hikita, T. Tamamura, *Macromol. Chem. Rapid Commun*., **6**, 375, 1985.
6. H.L. Wang, L.Toppare, J.E. Frenandez, "Conducting polymer blends: polythiophene and polypyrrole blends with polystyrene and poly(bisphenol A carbonate)", *Macromolecules*, **23**, 1053, 1990.
7. S.E. Lindsey, G.B. Street, *Synthetic Metals*, **10**, 67, 1985.
8. Y.H. Park, M.H. Man, *J. Appl. Polym. Sci*., **45**, 1973, 1992.

9. F. Selampinar, U. Akbulut, T. Yalchin, S. Suzer, L. Toppare, *Synthetic Metals*, **62**, 201, 1994.
10. F. Selampinar, U. Akbulut, E. Yildiz, A. Gungor, L. Toppare, "Synthesis of a novel poly(arylene ether ketone) and its conducting composites with polypyrrole", *Synthetic Metals*, **89**, 111, 1997.
11. F. Endres, G. Schwitzgebel, "Morphological and electrochemical studies of polypyrrole/Nafion", *Synthetic Metals*, **88**, 73, 1997.
12. M. Bardet, M. Guinaudeu, C. Bourgeoisat, H. Cherin, *Synthetic Metals*, **41-43**, 359, 1991.
13. F. Cèspedes, S. Alegret, "New materials for electrochemical sensingII. Rigid carbon-polymer biocomposites", *Trends in Analytical Chemistry*, **19**(4), 276-285, 2000.
14. A.M. Lowman, N.A. Peppas, "Hydrogels" In *Encyclopedia of Controlled Drug Delivery,* E. Mathiowitz, ed., Vol. 2, 397-418, John Wiley & Sons: New York, 1999.
15. Y.H. Arica, V.N. Hasirci, *Biomaterials*, **8**, 489, 1987.
16. V.V. Crosfet, M. Erdosy, T.A. Johnson, R.P. Buck, R.B. Ash, M.R. Neumann, "Microfabricated Sensor Arrays Sensitive to pH and K+ for Ionic Distribution Measurements in the Beating Heart", *Anal.Chem*., **67**, 1647, 1995.
17. N.F. Sheppard, Jr., M.J. Lesho, P. McNally, A.S. Francomacaro, "Microfabricated conductimetric pH sensor", *Sensors and Actuators B*, **28**, 95, 1995.
18. L. Li, D.R. Walt, "Dual-Analyte Fiber-Optic Sensor for the Simultaneous and Continuous Measurement of Glucose and Oxygen", *Anal.Chem.*, **67**, 3746, 1995.
19. S. Brahim, D. Narinesingh, A. Guiseppi-Elie, "Polypyrrole-hydrogel composites for the construction of clinically important biosensors", *Biosens Bioelectron*, **17**, 53-59, 2002.
20. S. Brahim, D. Narinesingh, A. Guiseppi-Elie, "Amperometric determination of cholesterol in serum using a biosensor of cholesterol oxidase contained within a polypyrrole-hydrogel membrane", *Anal Chim Acta*, **448**, 27-36, 2001.
21. S. Brahim, D. Maharajh, D. Narinesingh, A. Guiseppi-Elie, "Design and Characterization of a Galactose Biosensor using a Novel Polypyrrole-Hydrogel Composite Membrane" *Analytical Letters*, **35**(5), 797-812, 2002.
22. A. Witkowski, M.S. Freund, A. Brajter-Toth, "Effect of Electrode Substrate on the Morphology and Selectivity of Overoxidized Polypyrrole Films" *Anal. Chem*., **63**, 622-626, 1991.
23. M. Freund, L. Bodalbhai, A. Brajter-Toth, "Anion-Excluding Polypyrrole Films" *Talanta*, **38**, 95-99, 1991.
24. J. Wang , P. V. A. Pamidi, G. Cepria , S. Basak, K. Rajeshwar, "Overoxidized Poly{pyrrole-co-[3-(pyrrol-1-yl)-propanesulfonate]}-coated Platinum Electrodes for Selective Detection of Catecholamine Neurotransmitters" *Analyst*, **122**(9), 981-984, 1997.
25. P. A. Christensen, A. Hamnett, "In situ Spectroscopic Investigations of the Growth, Electrochemical Cycling and Overoxidation of Polypyrrole in Aqueous Solution", *Electrochimica Acta*, **36**(8), 1263-1286, 1991.
26. S.J. Martin, G.C. Frye, S.D. Senturia, "Dynamics and Response of Polymer-Coated Surface Acoustic Wave Devices: Effect of Viscoelastic Properties and Film Resonance" *Anal. Chem.* **66**, 2201-2219, 1994.
27. R. Lucklum, P. Hauptmann, "The $\Delta f$–$\Delta R$ QCM technique: an approach to an advanced sensor signal interpretation" *Electrochimica Acta* **45**, 3907-3916, 2000.

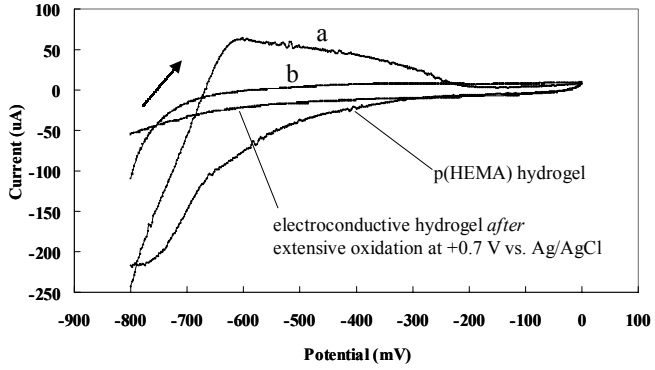


Figure 1. a) Cyclic voltammogram of cross-linked p(HEMA) hydrogel on platinized platinum IME 1025.5 in 0.1 M phosphate buffered KCl, pH 7.4. Scan rate = 20 mV/s. b) Cyclic voltammogram of electroconductive hydrogel composite on platinized platinum IME 1025.5 in 0.1 M phosphate buffered KCl, pH 7.4, after *2 hours* of extensive oxidation at +0.7 V *vs.* Ag/AgCl. Scan rate = 20 mV/s

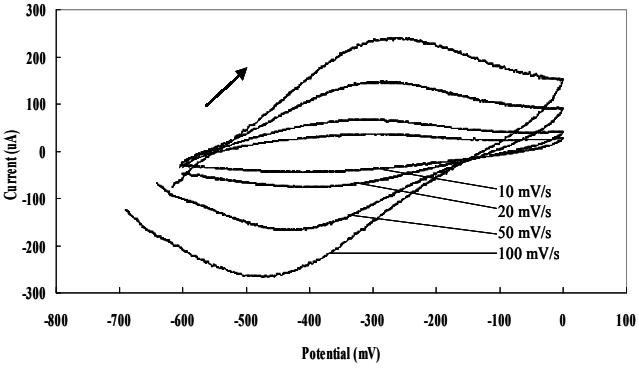


Figure 2. Cyclic voltammogram of polypyrrole on platinized platinum IME 1025.5 in 0.1 M phosphate buffered KCl, pH 7.4.

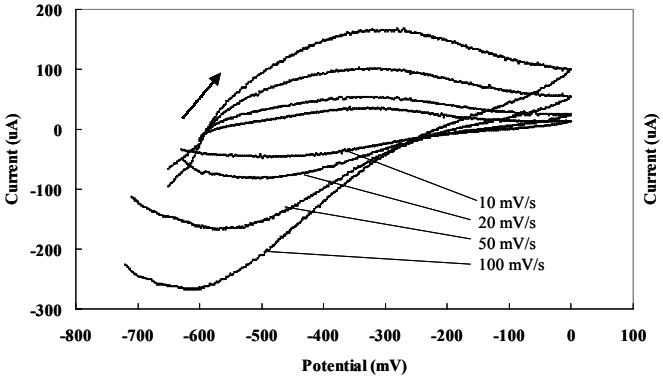


Figure 3. Cyclic voltammogram of electroconductive hydrogel composite on platinized platinum IME 1025.5 in 0.1 M phosphate buffered KCl, pH 7.4, *BEFORE* extensive oxidation.

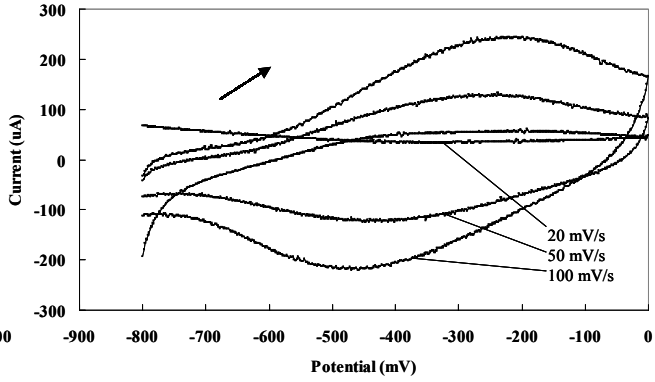


Figure 4. Cyclic voltammogram of electroconductive hydrogel composite on platinized platinum IME 1025.5 in 0.1 M phosphate buffered KCl, pH 7.4, after *1 hour* of extensive oxidation at +0.7 V *vs.* Ag/AgCl.

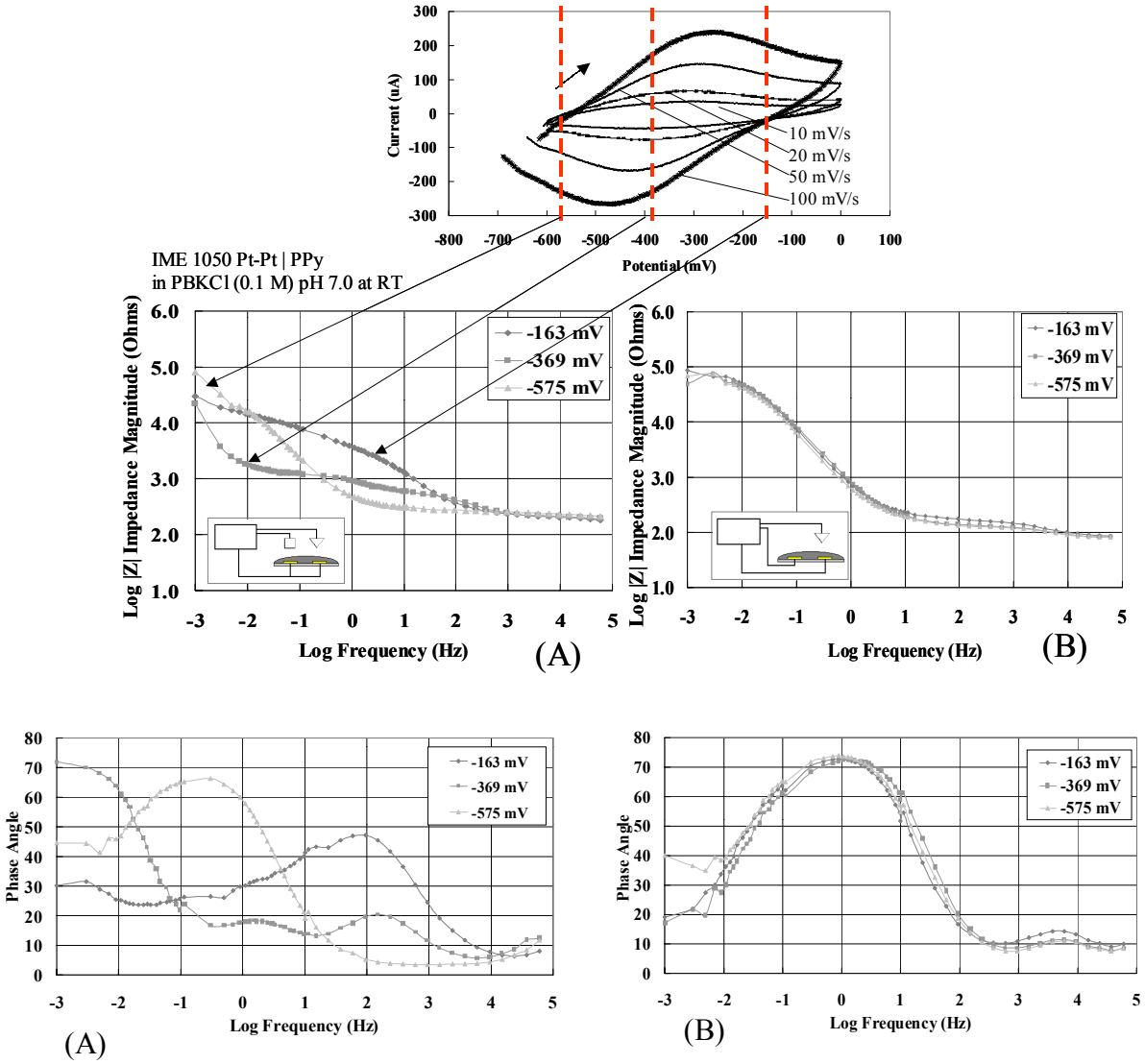


Figure 5.a) Bode plot of log real impedance magnitude *vs.* log frequency and phase angle *vs.* log frequency for *across* polypyrrole film on platinized platinum IME 1050 in 0.1 M phosphate buffered KCl, pH 7. b) Bode plot of log real impedance magnitude *vs.* log frequency and phase angle *vs.* log frequency for *within* polypyrrole film on platinized platinum IME 1050 in 0.1 M phosphate buffered KCl, pH 7.

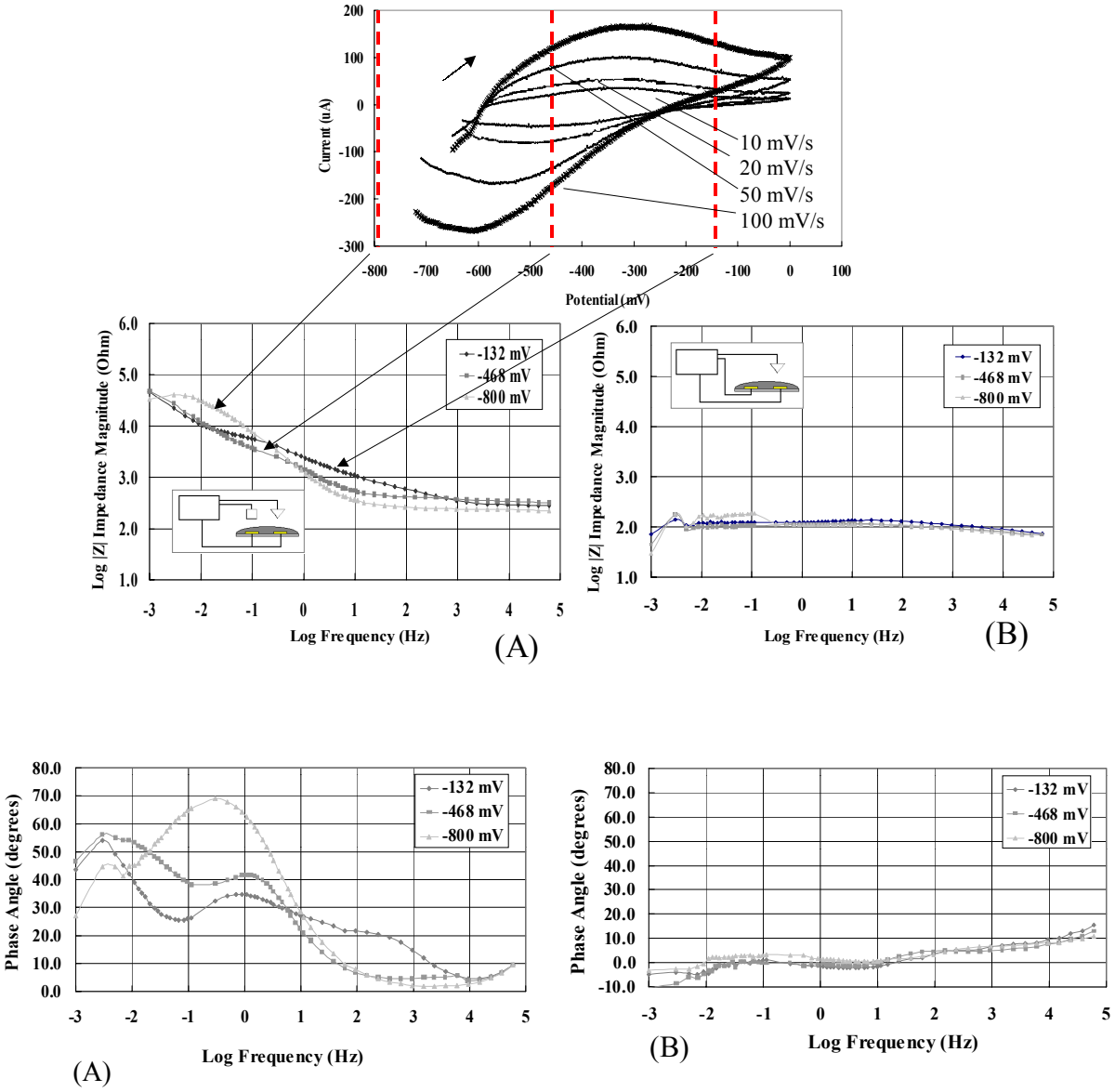


Figure 6. a) Bode plot of log real impedance magnitude *vs.* log frequency and phase angle *vs.* log frequency for *across* electroconductive hydrogel (*BEFORE* extensive oxidation) on platinized platinum IME 1050 in 0.1 M phosphate buffered KCl, pH 7. b) Bode plot of log real impedance magnitude *vs.* log frequency and phase angle *vs.* log frequency for *within* electroconductive hydrogel (*BEFORE* extensive oxidation) on platinized platinum IME 1050 in 0.1 M phosphate buffered KCl, pH 7.

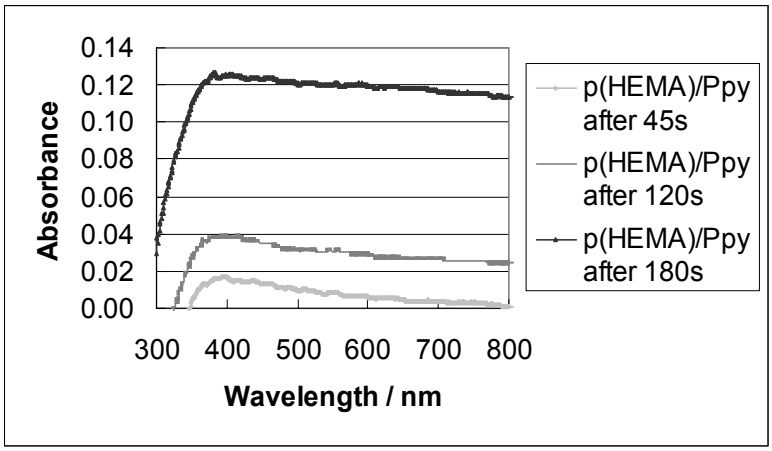


Figure 7. UV-Visible spectra of composite film of composition HEMA:TEGDA:Py (85:10:05 vol%) performed on indium-tin oxide plates over the wavelengths 300nm-800nm.

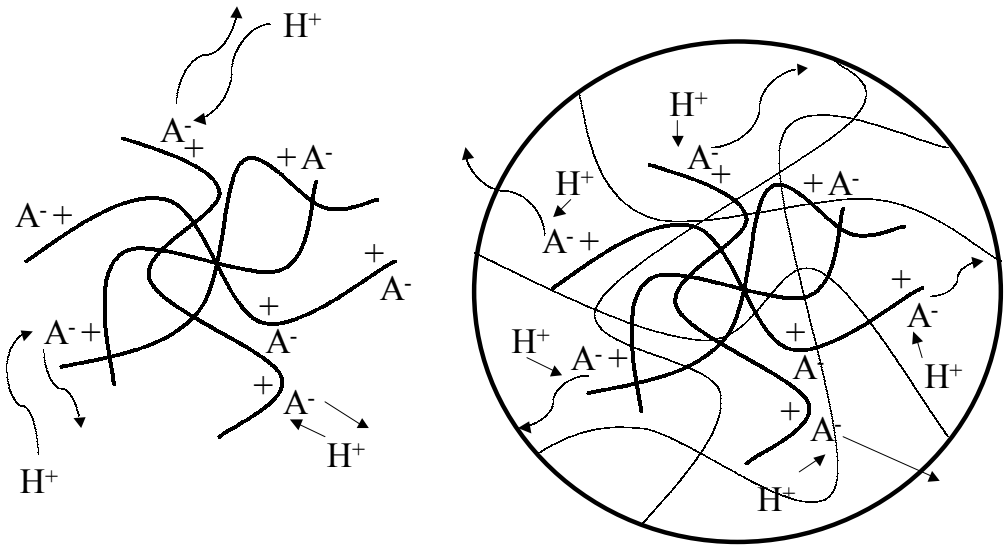


Figure 8. Schematic illustration of the swelling and ion exchange characteristics of PPy and PPy-p(HEMA) hydrogel composite.